frontiers in Energy Research

ORIGINAL RESEARCH
published: 28 January 2022
doi: 10.3389/fenrg.2022.828836

Exploring NH_3 and NO_x Interaction Chemistry With CH_4 and C_2H_4 at Moderate Temperatures and Various Pressures

Yuwen Deng[1], Zijian Sun[1], Wenhao Yuan[1], Jiuzhong Yang[2], Zhongyue Zhou[1] and Fei Qi[1]*

[1]School of Mechanical Engineering, Shanghai Jiao Tong University, Shanghai, China, [2]National Synchrotron Radiation Laboratory, University of Science and Technology of China, Hefei, China

The oxidation of $CH_4/C_2H_4/NH_3/NO/NO_2$ gas mixtures was studied aiming to explore the homogenous chemistry of exhaust gas from lean-operated natural gas engine. With respect to this goal, experiments were carried out with a laminar flow reactor under engine-relevant (diluted and lean) conditions over the temperature range of 600–1400 K. Four gas mixtures were designed to evaluate the effects of NO/NO_2 ratio (1, 4) and pressure (0.04 and 1.0 atm) on the interaction chemistry of NH_3/NO_x with CH_4 and C_2H_4. By using synchrotron vacuum ultraviolet photoionization mass spectrometry, fingerprint products for revealing interaction chemistry were identified and quantified, e.g., nitrogenous and oxygenated intermediates. The experimental results show that the NO concentrations are significantly affected by adding CH_4/C_2H_4, changing NO/NO_2 ratio and pressure. Besides, the promotion of $DeNO_x$ reactions and narrower temperature windows of NO reduction are unexpectedly observed in the presence of CH_4/C_2H_4. To interpret the experimental observations, a detailed kinetic model was developed by integrating hydrocarbons/NH_3/NO_x interaction chemistry. Rate of production and sensitivity analyses indicate that the active radical pool is enriched and additional chain-branching pathways regarding NO/NO_2 interconversion are activated with the addition of hydrocarbons. In the presence of both CH_4 and C_2H_4, reaction $C_2H_3 + O_2 = CH_2CHO + O$ was demonstrated as a crucial reaction that drives the reactivity of $CH_4/C_2H_4/NH_3/NO/NO_2$ mixture. This is explained by the production of CH_2CHO, whose dissociation generates CH_2O and ultimately leads to the abundant production of active OH *via* the reaction sequence $CH_2O \rightarrow HCO \rightarrow HO_2 \rightarrow OH$. The conversion kinetics of hydrocarbons, NO and NH_3 under different NO/NO_2 ratios and pressure, as well as the formation kinetics of oxygenated and nitrogenous intermediates was also analyzed in this work.

Keywords: nitrogenous oxides, ammonia, hydrocarbons, flow reactor oxidation, kinetic modeling

OPEN ACCESS

Edited by:
Zhihua Wang,
Zhejiang University, China

Reviewed by:
Bin Yang,
Tsinghua University, China
Yingjia Zhang,
Xi'an Jiaotong University, China

****Correspondence:***
Wenhao Yuan
yuanwh@sjtu.edu.cn

Specialty section:
This article was submitted to Advanced Clean Fuel Technologies, a section of the journal Frontiers in Energy Research

Received: *04 December 2021*
Accepted: *11 January 2022*
Published: *28 January 2022*

Citation:
Deng Y, Sun Z, Yuan W, Yang J, Zhou Z and Qi F (2022) Exploring NH_3 and NO_x Interaction Chemistry With CH_4 and C_2H_4 at Moderate Temperatures and Various Pressures. Front. Energy Res. 10:828836. doi: 10.3389/fenrg.2022.828836

1 INTRODUCTION

Modern combustion engine technologies have increasingly focused on the reduction of carbon dioxide emissions owing to the globally tightening legislation (Johnson, 2015; Börnhorst and Deutschmann, 2021), whereas the highly optimized engine structures and emission control measures render it extremely difficult to further make a breakthrough on decreasing raw

emissions. Meanwhile, lean-operated natural gas engines are considered as a promising technology because of their high thermo-efficiency and comparably low pollutant emissions (Lott and Deutschmann, 2021). Alternative concepts like biomethane and power-to-gas technologies will endow gas engines with outstanding potential on the way towards carbon neutrality (Schmitt et al., 2021). Nevertheless, the excessive engine-out emissions of methane, known with potent greenhouse potential and liable to produce carcinogenic formaldehyde by partial oxidation, bring new challenges to natural gas engines (Hutter et al., 2018). Also, the presence of nitrogen oxides (NO_x) in exhaust gas deserves special attention given its particular environmental hazard in engendering photochemical smog and acid rain (Gasnot et al., 2012; Piumetti et al., 2016). Hence, a highly efficient and durable exhaust gas abatement system, commonly containing both catalytic oxidation of unburned hydrocarbons (UHC) and NO_x reduction sections, was considered imperative (Lott and Deutschmann, 2021). The ammonia-based selective catalytic reduction (SCR) technology is currently widely applied for NO_x removal from gas engines benefiting from its higher $DeNO_x$ efficiency and relatively moderate cost. However, it must be pointed out that despite the whole $DeNO_x$ process integrating simultaneously complex gas-phase and surface chemistry (Vassallo et al., 1995; Tamm et al., 2009), the probability of the gas-phase reactions between hydrocarbons, NO_x and NH_3 in SCR was exclusively ignored among most of the studies regarding exhaust gas abatement (Mejía-Centeno et al., 2013; Wang et al., 2019; Lee et al., 2020; Jia et al., 2021; Savva et al., 2021), especially given the recently proposed post-treatment measures allowing the catalytic converters to be positioned closer to the engine thus featuring much higher pressure and temperatures (Lott and Deutschmann, 2021).

To the best of our knowledge, only limited studies have been reported to date in terms of the homogeneous reactivities of NH_3 and NO_x in the presence of multiple other typical exhaust gas constituents, mainly C_1-C_2 hydrocarbons like methane and ethylene, etc. Hemberger et al. (Hemberger et al., 1994) investigated the selective non-catalytic reduction (SNCR) of NO by ammonia with the addition of methane and ethane in a flow reactor over the temperature range 800–1300 K. Gasnot et al. (Gasnot et al., 2012) performed an experimental and kinetic study of the effect of several additives such as CH_4, C_2H_4, C_2H_6, C_2H_2, CH_3OH, C_2H_5OH and CO on ammonia-based SNCR process at temperatures of 900–1200 K. Torkashvand et al. (Torkashvand et al., 2019) investigated hydrocarbon abatement from the exhaust of lean-burn gas engines under ambient pressure and pre-turbine conditions. Most recently, Schmitt et al. (Schmitt et al., 2021) conducted flow reactor experiments in the temperature range of 700–1200 K at atmospheric pressure to reveal influences of individual components by adding NO_2, CH_4, CO, and C_2H_4 sequentially to a highly argon-diluted NO/NH_3 base mixture.

The aim of the present work is to explore the impact of methane and ethylene on the homogeneous conversion chemistry of NO_x and NH_3 under near-real exhaust conditions. With respect to this goal, the oxidation experiments of $CH_4/C_2H_4/NH_3/NO/NO_2$ gas mixtures were firstly carried out in a laminar flow reactor at lean conditions, at temperatures of 600–1400 K and pressures of 0.04–1.0 atm. Different gas mixtures were designed to investigate the impact of NO/NO_2 ratio and pressure on the conversion kinetics of NH_3, NO and hydrocarbons. Mole fraction profiles of reactants, products, hydrocarbon, nitrogenous and oxygenated intermediates were evaluated by using synchrotron vacuum ultraviolet photoionization mass spectrometry (SVUV-PIMS). On the basis of these experiments, a detailed kinetic model was developed to interpret the experimental results and reveal the conversion kinetics of NH_3 and NO_x in the presence of CH_4 and C_2H_4 under different conditions.

2 EXPERIMENTAL METHODS

The experimental work was conducted at the National Synchrotron Radiation Laboratory, China. Details about the experimental setup have been introduced in our previous work (Qi, 2013; Zhou et al., 2016). Four experimental conditions were selected to cover the pressure ranges from 0.04 to 1 atm, the temperature ranges from 600 to 1400 K, and different NO/NO_2 ratios. Detailed experimental conditions are listed in **Table 1**. Furthermore, two gas mixture conditions in the absence and presence of methane (Sun et al., 2021), which were reported previously, are also summarized in **Table 1** and will be discussed in the following sections to clarify the impact of individual gas additives on the conversion chemistry of NH_3/NO_x. The gas mixtures were highly diluted in carrier gas argon with a total flow rate of 250 standard cubic centimeters per minute (sccm) and an average residence time of 0.6–1.4 s. Gas mixtures were fed into a quartz flow reactor with 0.7 cm inner diameter and 40 cm heating length. The identification and quantification of intermediate species were achieved by using SVUV-PIMS. The calculated uncertainties of mole fractions for species with known photoionization cross sections (PICSs) were estimated to be ±25% and a factor of 2 for those with estimated PICSs.

3 KINETIC MODELING

The kinetic model used for the simulation was developed based on AramcoMech 3.0 (Zhou et al., 2018), which contains a well-established C_0-C_2 base mechanism. The sub-mechanism describing NH_3 oxidation as well as interaction kinetics between C_0-C_2 species and NO_x was taken from the work of Glarborg et al. (Glarborg et al., 2018). In addition, rate constants of several key reactions in the sub-mechanism of NH_3, which are mainly related to the production of NH_2 and NO, have been updated from the theoretical studies of Stagni et al. (Stagni et al., 2020). These reactions include the dissociation of HNO and H-abstraction reactions of NH_3 by H, O, OH and HO_2 radicals. The newly proposed reactions pathways of NH radicals by Duynslaegher et al. (Duynslaegher et al., 2012), namely the reactions of NH with O or N_2O to produce N + OH or N_2 + HNO, and the reaction of NH_2 with NO yielding

TABLE 1 | Experimental conditions.

Gas mixture	P/atm	CH_4/ppm	C_2H_4/ppm	NH_3/ppm	NO/ppm	NO_2/ppm	O_2	Ar
GM1	0.04	6,000	6,000	1,000	500	500	0.06	0.926
GM2	1	6,000	6,000	1,000	500	500	0.06	0.926
GM3 (Sun et al., 2021)	1	6,000	0	1,000	500	500	0.06	0.932
GM4 (Sun et al., 2021)	1	0	0	1,000	500	500	0.06	0.938
GM5	0.04	6,000	6,000	1,000	800	200	0.06	0.926
GM6	1	6,000	6,000	1,000	800	200	0.06	0.926

$N_2O + H_2$, etc., were also implemented in the present kinetic model. The rate constant of $NH_2 + O = HNO + H$ calculated by Sumathi et al. (Sumathi et al., 1998) was also adopted to improve the prediction results of NO_x. The detailed updating list of the rate constants involved in the C_1-C_2/NO_x/NH_3 sub-mechanism has been summarized in our recent work on CH_4/NH_3/NO_x (Sun et al., 2021), thus not outlined here.

Meanwhile, the C_1-C_2/NO_x/NH_3 sub-mechanism has also been further improved in the present work to describe the interaction kinetics among hydrocarbon species, NH species and NO_x. The reaction pathways of carbonyl species such as acrolein, acetaldehyde and ketene with NO_x, and the $C_2H_4 + NO_2$ channel laid out by Deng et al. (Deng et al., 2019) were included in the present model. Also, the recombination reactions of CH_3 and NH_2, together with C_2H_3 and NO/NO_2/CN, are implemented from the calculation results of Deng et al. (Deng et al., 2019) or by analogy with similar reactions when available. The reaction pathways describing the interaction chemistry between C_2H_2 and NO_x were taken from the recent studies of Marshall et al. (Marshall et al., 2019). Thermodynamic parameters of newly added species such as $CH_3NH2CH_3NO_2$, $C_2H_3NO_2$ and C_2H_3CN, etc. in the present model were taken from Glarborg et al. (Glarborg et al., 2018) and the theoretical calculations of Deng et al. (Deng et al., 2019). The simulation of flow reactor was carried out by using the Plug Flow Reactor module in Chemkin-Pro software (ReactionDesign, 2009) with the measured centerline temperatures of flow reactor as input parameters.

4 RESULTS AND DISCUSSION

Dozens of species were detected in the oxidation of CH_4/C_2H_4/NH_3/NO/NO_2 gas mixtures and their mole fractions were evaluated as functions of temperatures. Specifically, major nitrogenous intermediates detected and identified in this work include nitromethane (CH_3NO_2), nitroethylene ($C_2H_3NO_2$), methylamine (CH_3NH_2), nitrous acid (HONO) and cyanides (HCNO). Major oxygenated intermediates detected include formaldehyde (CH_2O), methanol (CH_3OH) and acetaldehyde (CH_3CHO). In the following sections, effect of CH_4/C_2H_4 on the NO_x/NH_3 homogeneous conversion chemistry will be discussed first. Subsequently, the impacts of pressure and NO/NO_2 ratio on the kinetics of HCs/NO_x/NH_3 mixture will be analyzed. Finally, the formation kinetics of nitrogenous and oxygenated intermediates will be analyzed to reveal the unique interactive reactions among hydrocarbons, NH_3 and NO_x.

4.1 Effect of CH_4 and C_2H_4 Addition on NO_x/NH_3 Conversion

Figure 1 shows the experimental and predicted mole fraction profiles of reactants (NH_3, NO, NO_2 and O_2) in the oxidation of gas mixtures 1–6 (GM1-6), **Figure 2** shows the experimental and simulated mole fraction profiles of major products (N_2O, N_2, H_2O, CO and CO_2) in the oxidation of GM1-3 and GM5-6. For all the investigated gas mixtures, the model is capable of predicting the temperature-dependent decomposition profiles of reactants except for the discrepancy observed for NO in GM1 and GM4. Regarding the major products, the model is able to reproduce the formation of most products except that the under-estimation of equilibrium concentration of N_2 at 0.04 atm. Rate of production (ROP) analyses have been carried out to reveal the conversion kinetics of NO_x and NH_3 under different conditions. The selected temperatures for the ROP analyses, i.e., 1239 K (GM1), 886 K (GM2), 911 K (GM3), 1060 K (GM4) and 1239 K (GM5), correspond to the temperature at which the conversion rate of ammonia reaches about 50%.

Numerous previous studies (Miller and Bowman, 1989; Glarborg et al., 2018; Okafor et al., 2018; Schmitt et al., 2021) have concluded that reactions R1-R5 are the major reactions in the oxidation of NH_3/NO_x. **Figure 3** summarizes the reaction pathways of NH_3 in the oxidation of GM1-5. The results show that regardless of whether there is the addition of hydrocarbons, over 90% of NH_3 is converted to NH_2 *via* H-abstraction reaction by OH. In the oxidation of NH_3/NO_x (GM4), reactions R2 and R4 contribute to a major part of NH_2 consumption, producing N_2 and nitroxide (H_2NO), respectively. The remaining two reactions R1 and R5 produce NNH and N_2O, respectively. NNH and N_2O are eventually converted to N_2 through single-step collision reactions. H_2NO produced from R4 is eventually converted to NO *via* nitroxyl (HNO) through stepwise dehydrogenation reactions.

$$NH_2 + NO = NNH + OH \quad (R1)$$

$$NH_2 + NO = N_2 + H_2O \quad (R2)$$

$$NO + HO_2 = NO_2 + OH \quad (R3)$$

$$NH_2 + NO_2 = H_2NO + NO \quad (R4)$$

$$NH_2 + NO_2 = N_2O + H_2O \quad (R5)$$

By examining **Figure 3** one can see that the profile of NO with temperature in GM4 has a distinct difference from that in other mixtures, and is also different from the result observed in the work of Schmitt et al. (Schmitt et al., 2021). To clarify the kinetics

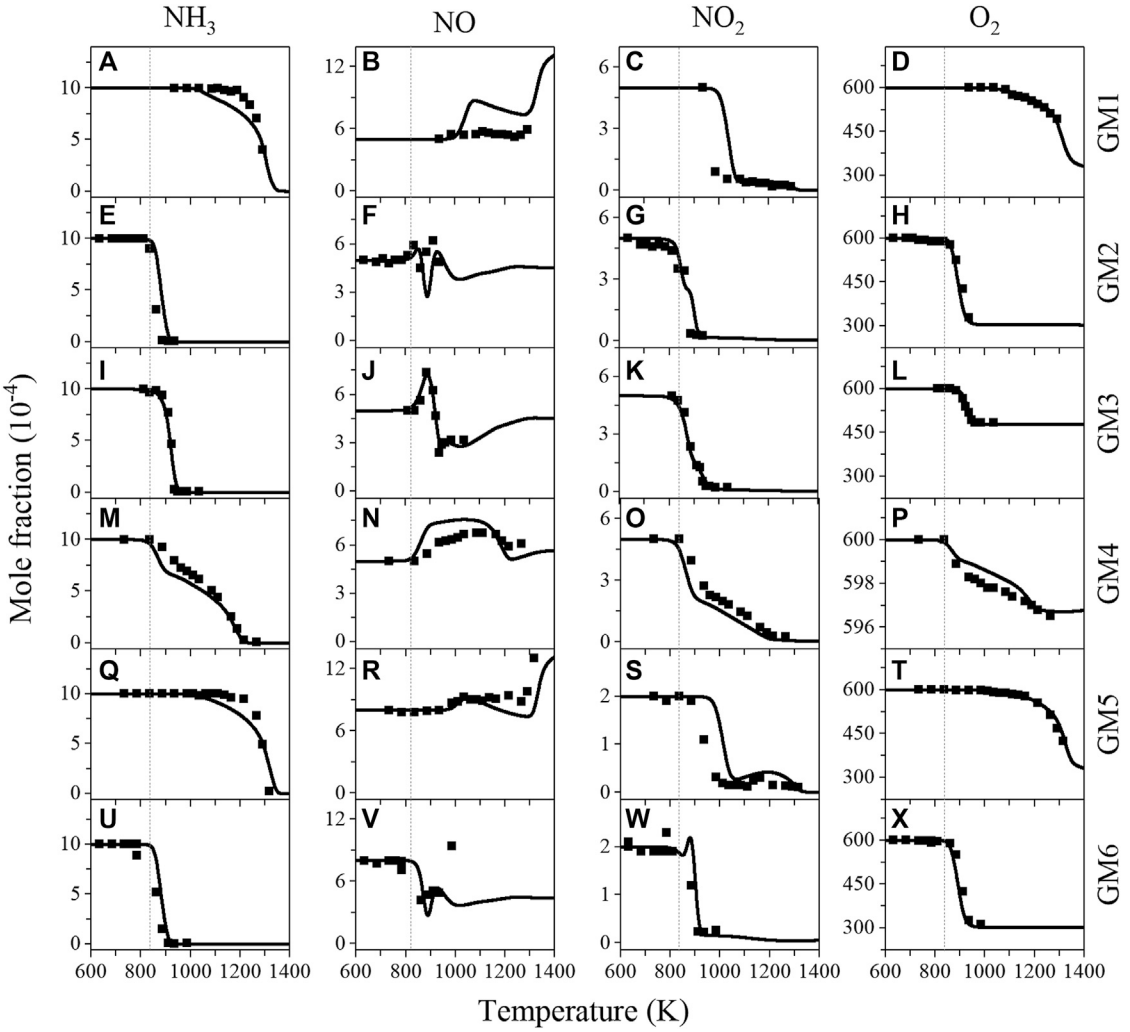

FIGURE 1 | Experimental (symbols) and simulated (lines) mole fraction profiles of ammonia (NH_3), nitric oxide (NO), nitrogen dioxide (NO_2) and oxygen (O_2) from the oxidation of GM1-6. Experimental data of GM3-4 are taken from the work of Sun et al. (Sun et al., 2021).

behind it, ROP analyses were performed at low- to high-temperatures (860, 1,162 and 1316 K). The results indicate that the initial increase of NO at the temperature of 863 K is mainly caused by the decomposition of nitrous acid (HONO), followed by the interconversion reaction R4. HONO is produced through the reaction sequence $NH_2 \rightarrow H_2NO \rightarrow HNO\ (+NO_2) \rightarrow HONO$. Over the temperature range of 900–1100 K, the concentration of NO has only a slight change, generally because the thermal $DeNO_x$ reactions R1 and R2 proceed rather slow over this temperature range. When the temperature increases above 1100 K, NO is quickly consumed *via* the thermal $DeNO_x$ reactions R1 and R2. As the temperature increases up to 1300 K, a second rise of NO concentration with temperature is observed. ROP analysis results show that reaction R6 is the dominant reaction that contributes to the formation of NO at temperatures above 1300 K.

$$NO_2 + H = NO + OH \quad \text{(R6)}$$

In comparison with the oxidation of NH_3/NO_x (GM4), no noticeable change was observed for the initial conversion temperatures of NH_3 and NO_x in the oxidation of $CH_4/NH_3/NO_x$ (GM3). However, in the presence of both CH_4 and C_2H_4 (GM2), the initial conversion temperatures of NH_3 and NO_x are found around 50 K lower than those in the oxidation of NH_3/NO_x, as seen in GM2, 3, 4 in **Figure 1**. By comparing GM2, GM3, GM4 and GM6, it can be also concluded that the addition of hydrocarbons promotes the consumption rate of NH_3, NO_2 and O_2, i.e., for GM2, GM3 and GM6, NH_3, NO_2 and O_2 are quickly consumed over a narrow temperature range, while for GM4, the temperature regime is much wider.

The comparison of experimental and simulated mole fraction profiles of CH_4 and C_2H_4 in GM1-3 and GM5-6 is illustrated in **Figure 4**. As expected, the initial conversion temperatures, as well as reaction temperature regime of CH_4 and C_2H_4 are noticeably affected by the NO/NO_2 ratio and the pressure. To elucidate the effect of CH_4/C_2H_4 addition on NO reduction, sensitivity analysis

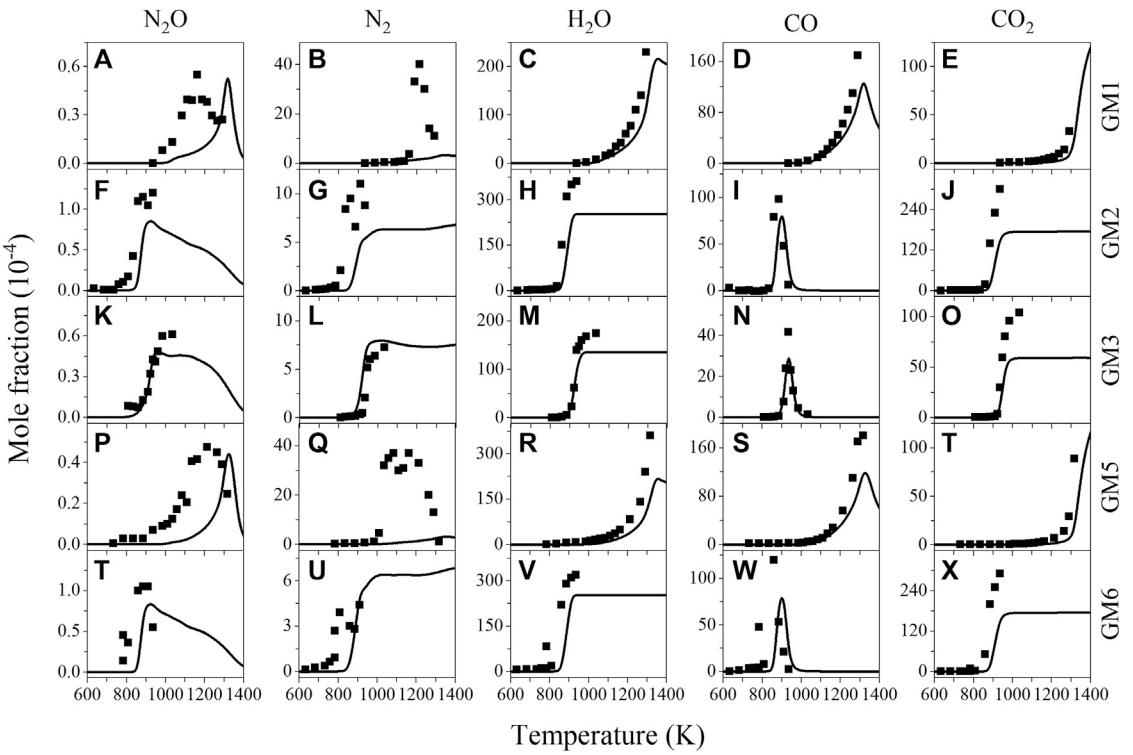

FIGURE 2 | Experimental (symbols) and simulated (lines) mole fraction profiles of nitrous oxide (N_2O), nitrogen (N_2), water (H_2O), carbon monoxide (CO) and carbon dioxide (CO_2) from the oxidation of GM1-3, GM5 and GM6. Experimental data of GM3 are taken from the work of Sun et al. (Sun et al., 2021).

on NO was also performed for GM1-4 and the results are summarized in **Figure 5**, a negative sensitivity coefficient indicates the promoting effect on NO consumption. As seen in **Figure 5D**, the competing reactions R1 and R2 show considerable sensitivity to NO consumption in GM4. Other sensitive reactions include chain-branching reactions promoting the formation of active radical pool along with those related to NO/NO_2 interconversion.

In the oxidation of $CH_4/NH_3/NO_x$ mixture (GM3), the concentration of NO has a first rise at a lower temperature (~ 860 K), and then it quickly decreases at the temperature around 911 K (**Figure 1J**). As the temperature increases to 1080 K, the concentration of NO has a second rise. According to the ROP analyses, the first rise of NO concentration is attributed by the reaction of CH_3 and NO_2 (R7). The reduction of NO between 911–1080 K is attributed by the thermal $DeNO_x$ reactions (R1 and R2), the interaction between NO and HO_2 (R3), and the reaction of CH_3O with NO (R8). The second rise of NO at higher temperatures is attributed by the reaction R6, which is the same as that in the oxidation of GM4. The sensitivity analyses shown in **Figure 5C** again illustrate the crucial role of reactions R7 and R8, i.e., converting the relatively inactive CH_3 and CH_3O_2 into highly active and unstable CH_3O radicals. The decomposition of CH_3O radical initiates the chain-branching reaction by replenishing the active radical pool to a major extent *via* the reactions $CH_3O(+M) = CH_2O + H(+M)$ and $H + O_2 = OH + O$. In addition, another consumption pathway of CH_3O, i.e., $CH_3O + O_2 = CH_2O + HO_2$, produces HO_2 of lower reactivity and competes with the above-mentioned direct dehydrogenation channel, thus exhibiting negative sensitivity to the reduction of NO.

$$CH_3 + NO_2 = CH_3O + NO \quad (R7)$$

$$CH_3O_2 + NO = CH_3O + NO_2 \quad (R8)$$

In the presence of both CH_4 and C_2H_4 (GM1-2, GM5-6), the reaction network becomes more complex. Base on the ROP analysis, the reaction scheme is summarized in **Figure 6**. It should be noted that for all the four gas mixtures the major reaction pathways are similar, while the reaction flux is different. In the case of CH_4/C_2H_4 addition, the mole fraction profiles of NO in GM2 also show multiple extreme points. ROP analyses at 835, 860, 911, and 985 K suggests that the occurrence of the first maximum and minimum points of NO mole fraction is the same as GM3 in terms of the kinetic interpretation, while the following attenuation of NO is dominated by the oxidation reaction with HO_2 (R3), while other reactions have little impacts on it. Additionally, for the low pressure case of GM1 (0.04 atm), the reduction of NO is not sensitive to the recombination of methyl or vinyl group with NO_2, which is in clear contrast to GM2.

According to the ROP analyses, CH_4 mainly proceeds the H-abstraction reaction initiated by OH to produce CH_3, which is further oxidized by NO_2 or HO_2 producing methoxyl, or undergoes the recombination reactions with NO_2, O_2 and CH_3. Particularly, the recombination reaction of CH_3 and NO_2

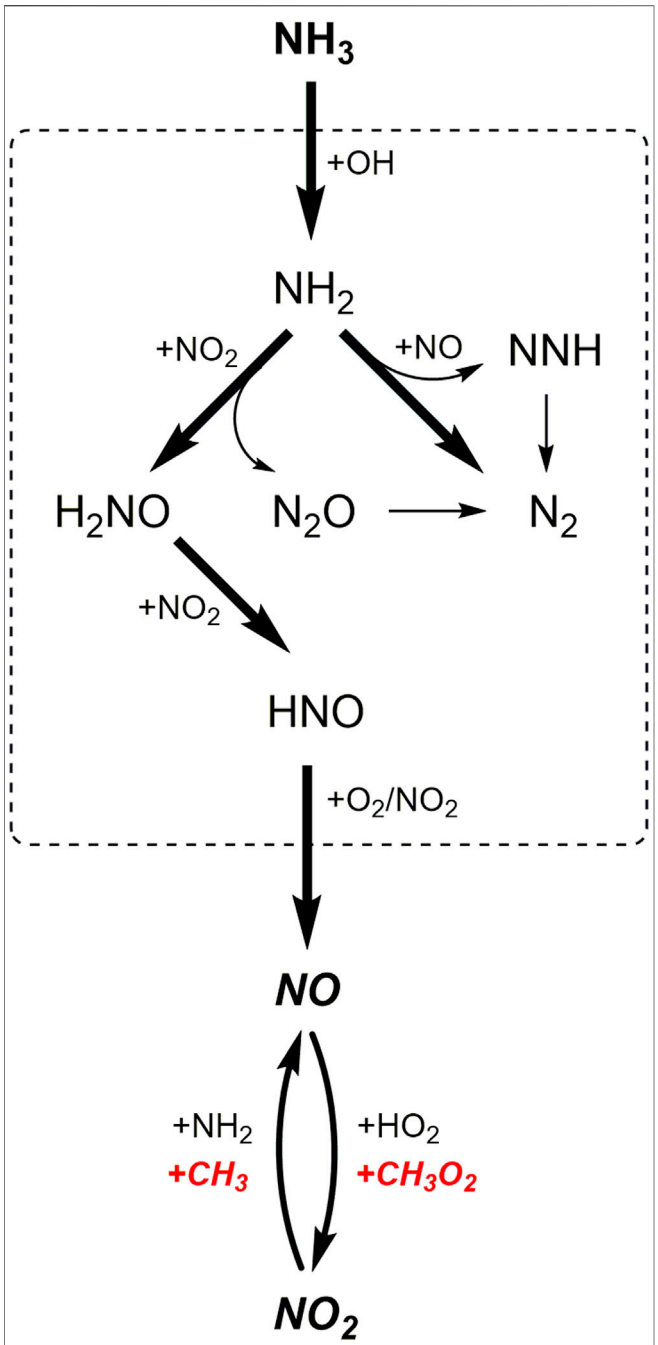

FIGURE 3 | Major reaction paths of NH_3 in the oxidation of GM1, GM2, GM3, GM4, GM5 and GM6.

(R9) is a major reaction that inhibits the reduction of NO, as can be seen in **Figure 5B**, while the competing oxidizing reaction R7 is the dominant reaction that promotes the consumption of NO. CH_3O subsequently decomposes to CO through CH_2O and HCO *via* the stepwise H-elimination process, CO is mainly converted to CO_2 *via* the reaction CO + OH = CO_2+H.

$$CH_3NO_2\,(+M) = CH_3 + NO_2\,(+M) \qquad (R9)$$

At low pressure, the consumption of C_2H_4 mainly undergoes the H-abstraction reaction by OH, giving vinyl radical (C_2H_3). At atmospheric pressure, OH-addition reaction producing 2-hydroxyethyl (PC_2H_4OH) also becomes important. PC_2H_4OH prefers to add O_2 to form $O_2C_2H_4OH$, which further dissociates into two formaldehyde molecules *via* the C-C bond fission reaction. The consumption pathways of C_2H_3 are more complex than those of PC_2H_4OH. On one hand, C_2H_3 can add O_2 or NO, followed by β-C-C scission reaction and finally produce formaldehyde. On the other hand, it can take an O atom from O_2 (R10) or NO_2 (R11) to form vinoxy (CH_2CHO). Besides, part of C_2H_3 undergoes recombination reaction with NO_2 (R12) and this reaction is the most sensitive reaction that promotes the reduction of NO at 1 atm, as shown in **Figure 5B**. Reaction R12 is a typical competitive reaction of R7 (CH_3 + NO_2 = CH_3O + NO), which is the most sensitive reaction that inhibits the reduction of NO. Therefore, in the presence of both CH_4 and C_2H_4, the role of CH_4 and C_2H_4 on the reduction of NO is opposite. This can be also proved by the extremely slight change of NO reduction ratios as well as the $DeNO_x$ temperature windows of GM2 and GM3 shown in **Figure 1**. Although the subsequent reaction of ethylene also involves interaction reactions with NO_x, the proportion of this interaction is not appreciable (mostly less than 5%).

$$C_2H_3 + O_2 = CH_2CHO + O \qquad (R10)$$

$$C_2H_3 + NO_2 = CH_2CHO + NO \qquad (R11)$$

$$C_2H_3NO_2 = C_2H_3 + NO_2 \qquad (R12)$$

As a key intermediate produced from the interaction between C_2H_4 and NO_x, CH_2CHO can either react with O_2 to produce CH_2O, or produce ketene (CH_2CO) *via* H-abstraction reaction by NO_2. It is noteworthy that CH_2O is also a major decomposition product of CH_3O. As a result, CH_2O is an abundant product in the oxidation of $CH_4/C_2H_4/NO_x/NH_3$ mixtures at atmospheric pressure The decomposition of CH_2O eventually produces active OH *via* the reaction sequence CH_2O $_{(+OH/H/O)}$ → HCO $_{(+O2)}$ → HO_2 $_{(+NO)}$ → OH and thereby promote the reactivity. The ketenyl (HCCO) radical produced by CH_2CO can either be directly converted to CO and CO_2, or proceed the reactions with NO/NO_2 leading to the formation of HCNO. A majority of HCNO undergoes the reaction with OH yielding CO, the remaining part decomposes to CO *via* the HCO as intermediate.

In general, the addition of CH_4/C_2H_4 at lean conditions promotes the formation of reactive radicals, thereby enhancing the global reaction reactivity. In addition, additional chain-branching pathways that consume NO are introduced due to the formation of CH- or CHO- type radicals such as CH_3O. As a result, in the presence of CH_4/C_2H_4, the NO conversion temperature regime is narrower than that in the oxidation of NH_3/NO_x, which is in agreement with the conclusions of Glarborg et al. (Glarborg et al., 2018).

4.2 Effects of NO/NO_2 Ratio and Pressure on $HCs/NO_x/NH_3$ Kinetics

4.2.1 CH_4 and C_2H_4

As can be observed in **Figure 4**, when NO/NO_2 ratio increases from 1 to 4, the initial decomposition temperature of C_2H_4 is only

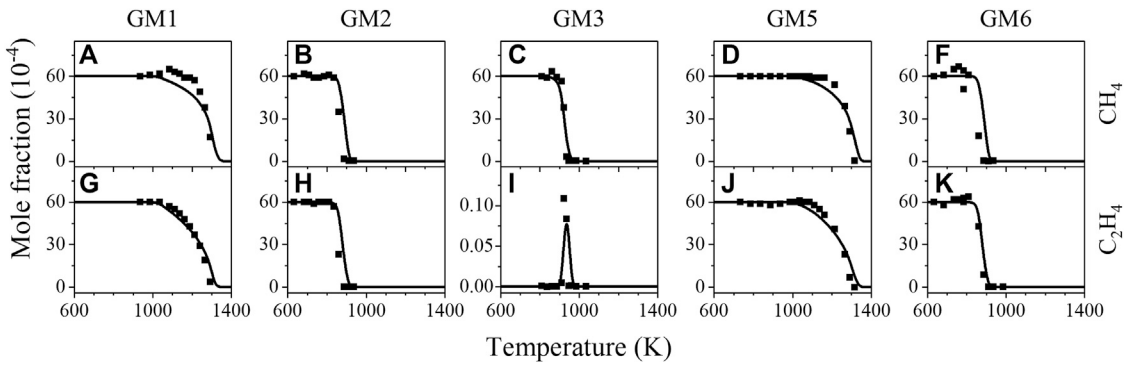

FIGURE 4 | Experimental (symbols) and simulated (lines) mole fraction profiles of methane (CH_4) and ethylene (C_2H_4) in the oxidation GM1, GM2, GM5 and GM6.

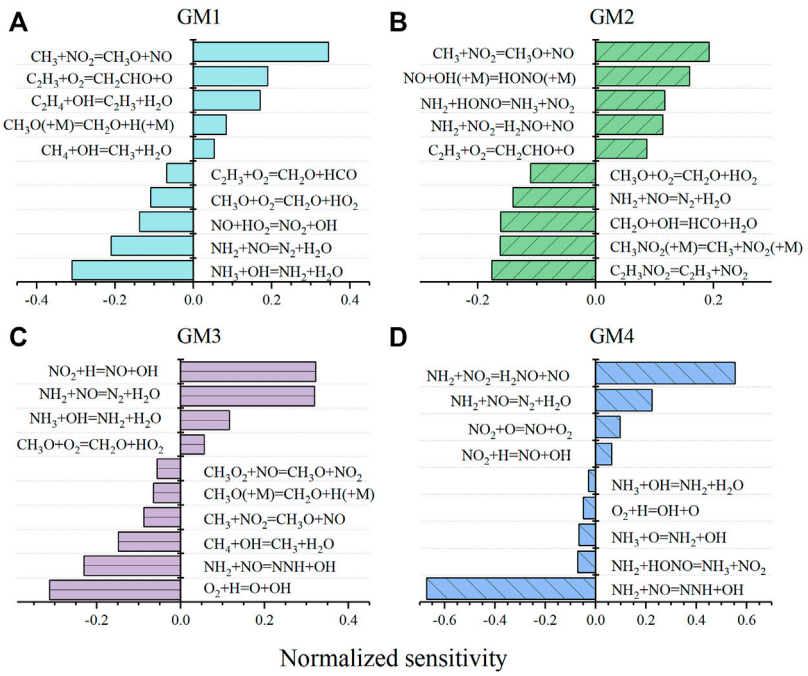

FIGURE 5 | Sensitivity analysis of NO during the flow reactor oxidation of GM1, GM2, GM3 and GM4 at 1213, 860, 911, and 1188 K, respectively. Negative sensitivity coefficients indicate promotion to NO consumption.

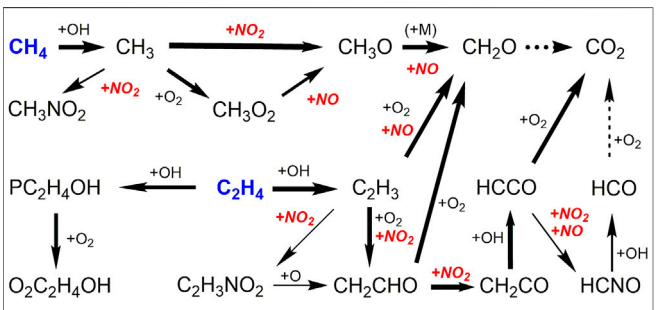

FIGURE 6 | Major reaction paths of CH_4 and C_2H_4 in the oxidation of GM1, GM2, GM5 and GM6 at 1239, 886, 1239, and 886 K, respectively.

slightly changed, while the initial decomposition temperature of CH_4 is decreased by around 50 K. As pressure increases from 0.04 to 1 atm, the initial decomposition temperatures of CH_4 and C_2H_4 are decreased by around 150–400 K. ROP and sensitivity analyses have been performed to clarify the influence of NO/NO_2 ratio and pressure on the conversion kinetics of CH_4 and C_2H_4. **Figure 7** displays the sensitivity analysis results of CH_4 and C_2H_4 in the flow reactor oxidation of GM1, GM2, GM5 and GM6 at 1239, 886, 1239, and 886 K, respectively. It can be seen that the dominant reactions have not changed significantly as the NO/NO_2 ratio increases from 1 to 4, indicating that the NO/NO_2 ratio has little effect on the conversion kinetics of CH_4 and C_2H_4.

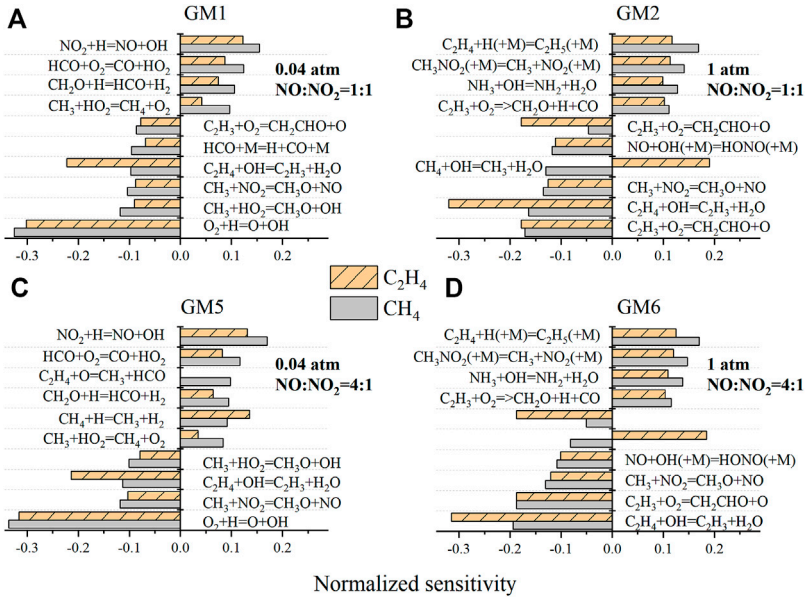

FIGURE 7 | Sensitivity analysis on CH_4 and C_2H_4 consumption during the flow reactor oxidation of GM1, GM2, GM5 and GM6 at 1239, 886, 1239, and 886 K, respectively.

In contrast to NO/NO_2 ratio, the change of pressure has significant effect on the dominant reactions of CH_4 and C_2H_4 consumption. As seen in **Figure 7**, at low pressure, the typical chain-branching reaction H + O_2 = OH + O is the most sensitive reaction promoting the consumption of CH_4 and C_2H_4. The reaction CH_3+NO_2 = CH_3O + NO is also identified as a sensitive promoting reaction. This does not seem surprising since this reaction and the following decomposition reactions of CH_3O have been already identified as one of the most important reactions that initiate the production of radical pool. At atmospheric pressure, H-abstraction reaction of C_2H_4 by OH is identified as the dominant reaction responsible for the consumption of both CH_4 and C_2H_4. H-abstraction reaction of CH_4 by OH is observed as a promoting reaction for CH_4 consumption but an inhibiting reaction for C_2H_4 consumption. This indicates that OH plays a key role in controlling the global reactivity. The O_2-addition reaction of C_2H_3 is also a sensitive promoting reaction for CH_4 and C_2H_4 consumption. As discussed above, the decomposition of CH_2CHO produced from this reaction readily generates CH_2O, whose further decomposition reaction produces HCO as major products.

4.2.2 NH_3 and NO

Figure 8 depicts the sensitivity analysis results of NH_3 during the flow reactor oxidation of GM1, GM2, GM5, and GM6 at 1239, 886, 1239, and 886 K, respectively. Similar to CH_4 and C_2H_4, the dominant reactions for NH_3 consumption are almost identical at different NO/NO_2 ratios. At low pressure (0.04 atm), the most sensitive reaction for NH_3 conversion is H + O_2 = O + OH owing to the relatively higher temperatures. At atmospheric pressure, H-abstraction reaction by OH controls the decomposition of NH_3. Reaction C_2H_4 + OH = C_2H_3 + H_2O and reaction C_2H_3 + O_2 = CH_2CHO also play a key role in the conversion of NH_3 regardless of low and atmospheric pressure, the latter reaction is closely related to the abundant production of CH_2O which ultimately dominates the yield of OH. Under both low and atmospheric pressure, the H-abstraction reaction of CH_4 by OH always plays the role that inhibits the conversion of NH_3, since CH_4 and its decomposition products strongly compete for the active radical pool (OH/O/H).

As can be observed in **Figure 1**, the maximum conversion ratio of NO increases as NO/NO_2 ratio increases. Besides, the impact of pressure on the conversion of NO is also significant. At atmospheric pressure the conversion ratio of NO increases (from 9% in GM2 increased to 45% in GM6) as NO/NO_2 ratio increases from 1 to 4. However, at low pressure (0.04 atm) the concentration of NO is found to go up with increasing temperature, i.e., at the same NO/NO_2 ratio, the fall of pressure directly inhibits the reduction of NO. In the oxidation experiment on $CH_4/NO/NO_2$ carried out by Sahu et al. (Sahu et al., 2021), it is also found that the initial NO fraction needs to approach a certain level to enhance the reactivity of the mixture, or else the low level of NO would act as an inhibitor. This non-monotonous sensitization impact of NO is attributed to the antagonism between chain-terminating reaction CH_3 + NO_2 (+M) = CH_3NO_2 (+M) and chain-branching process CH_2O + HO_2 = HCO + H_2O_2, H_2O_2(+M) = OH + OH(+M). Sahu et al. pointed out that when the initial concentration of NO is high, more CH_2O and HO_2 are produced, thus leading to the transition to chain-branching process.

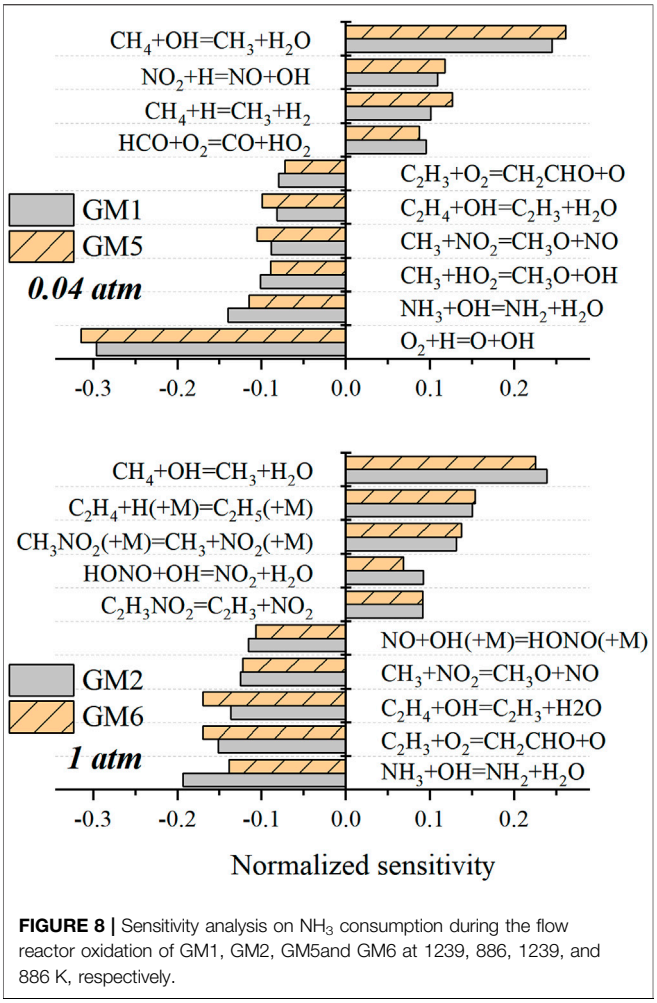

FIGURE 8 | Sensitivity analysis on NH_3 consumption during the flow reactor oxidation of GM1, GM2, GM5and GM6 at 1239, 886, 1239, and 886 K, respectively.

4.3 Formation of Major Products and Intermediates

N_2 and N_2O are two major nitrogenous products observed in the present work. As seen in **Figure 2**, the present model can capture the profiles of N_2 at atmospheric pressure, while highly under-predicts its formation at low pressure. Base on the sensitivity analysis, the formation of N_2 is controlled by reaction R7 (CH_3 + NO_2 = CH_3O + NO). However, the kinetics of CH_3 + NO_2 under low pressure remains controversial despite certain studies available in the literature (Yamaguchi et al., 1999; Srinivasan et al., 2005; Glarborg et al., 2018). Therefore, the under-estimation of N_2 at low-pressure may be attributed to the under-estimation of the rate constant of R7 at higher temperatures.

Glarborg et al. (Glarborg et al., 2018) mentioned that one of the disadvantages of SNCR with urea lies in the formation and possible emission of N_2O, which is a harmful gas destroying ozone layer. In the present experiments, N_2O has been observed to form in the order of tens of ppm on average over a wide temperature range. ROP analysis shows that almost all of N_2O is produced from reaction R5 (NH_2 + NO_2 = N_2O + H_2O) at atmospheric pressure, while at low pressure the reaction NH + NO = N_2O + H controls the formation of N_2O. In the work of Alzueta et al. (Alzueta et al., 2021), few ppm of N_2O formation was also detected in the flow reactor oxidation experiment of NH_3/NO, and the reaction N_2H_2 + NO = NH_2 + N_2O was considered as dominant reaction for N_2O formation. However, in the present work the contribution of this pathway is found almost negligible (<1%) for N_2O formation.

Figure 9 illustrates the experimental and simulated mole fraction profiles of CH_3OH, CH_2O and CH_3CHO in the oxidation of GM1, GM2, GM5 and GM6. Among them, CH_2O is the most abundantly produced. ROP analysis shows that the reaction $CH_3O(+M) = CH_2O + H(+M)$ dominates CH_2O formation independent of pressure and NO/NO_2 ratio. The production of CH_2O is derived from either methane- or ethylene-related oxidation steps. At atmospheric pressure, these two parts account for almost half of each, while at low pressure due to the activation of the additional formaldehyde generation path, $CH_3 + O = CH_2O + H$, the part derived from methane occupies about 70%. The concentration of CH_2O at low pressure peaks at a relatively high temperature of 1200 K, demonstrating that at this temperature it is sufficient to overcome the energy barrier of the reaction between CH_3 and O.

In regard to acetaldehyde (CH_3CHO), its production is closely related to ethenol (C_2H_3OH). At atmospheric pressure a majority of CH_3CHO is produced *via* the reaction $C_2H_3OH + NO/NO_2 = CH_3CHO + NO/NO_2$. At low pressure, most of CH_3CHO is formed from the isomerization of ethenol. As an unstable reactive intermediates, C_2H_3OH is primarily generated from the reaction $C_2H_4 + OH = C_2H_3OH + H$, and partly from the reaction $C_2H_4 + OH = CH_3CHO + H$. As for methanol, the yield observed in the experiment is not notable, mainly deriving from the H-abstraction of CH_3O from HO_2 or CH_2O, or through the recombination of CH_3 and OH.

Figure 10 displays the experimental and simulated mole fraction profiles of HCNO and HONO in gas mixtures of GM1, GM2, GM5 and GM6. HCNO is a key nitrogenous intermediate produced from the interaction of hydrocarbons and NO_x under high temperature and reducing conditions in reburning chemistry, where nitric oxides are converted into cyanides and isocyanides by reactions with multiple hydrocarbon-derived radicals such as CH_3, $^3CH_2$, and HCCO. Under the excess oxygen condition investigated in this work, part of the contribution of hydrocarbon derivatives to NO reduction is found mainly through the reactions R13-R15.

$$C_2H_3 + NO = HCN + CH_2O \quad (R13)$$

$$CHCHO + NO = HCNO + CO + H \quad (R14)$$

$$HCCO + NO = HCNO + CO \quad (R15)$$

The above reactions contribute less than 1% to NO reduction at atmospheric pressure, but at low pressure, it approaches around 9%. Consequently, although the addition of CH_4/C_2H_4 enriches the free radical pool and promotes the reactivity of the NH_3/NO/NO_2 mixture, its direct contribution to NO reduction is still negligible compared to the thermal $DeNO_x$ reactions (R1-R5). Furthermore, R13-R15 mostly feed into the cyanide pool (HCN,

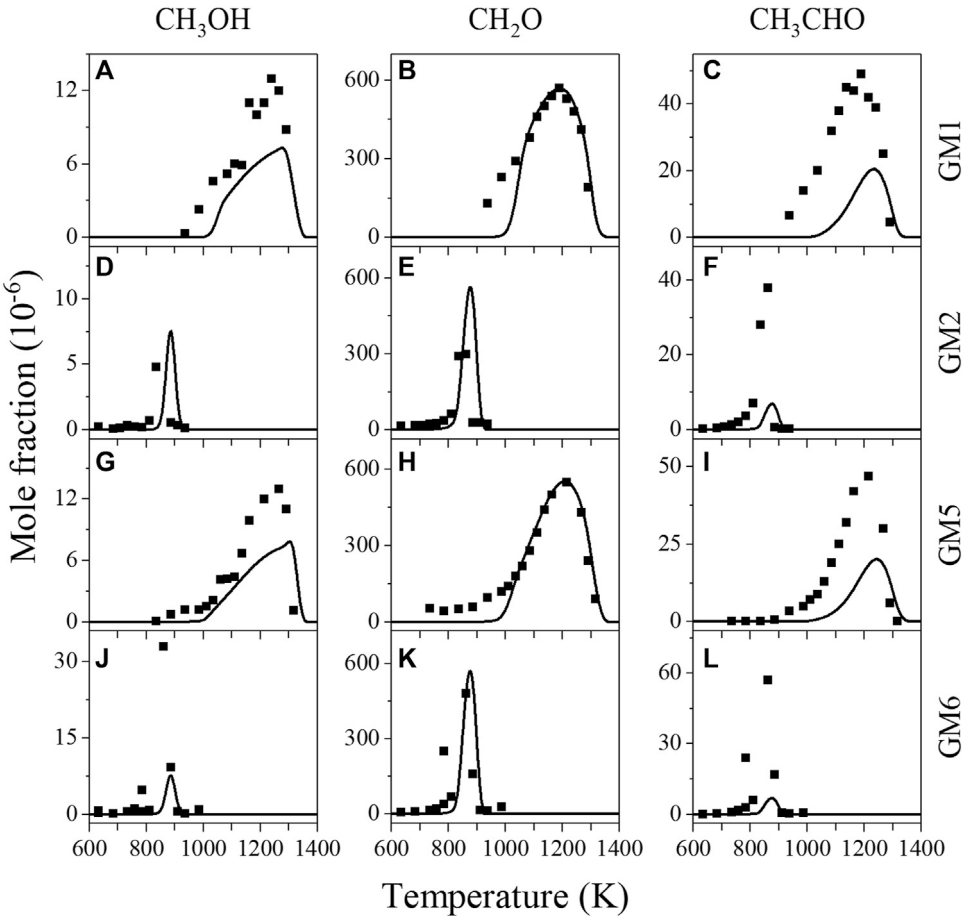

FIGURE 9 | Experimental (symbols) and simulated (lines) mole fraction profiles of methanol (CH_3OH), formaldehyde (CH_2O) and acetaldehyde (CH_3CHO) in the oxidation of GM1, GM2, GM5 and GM6.

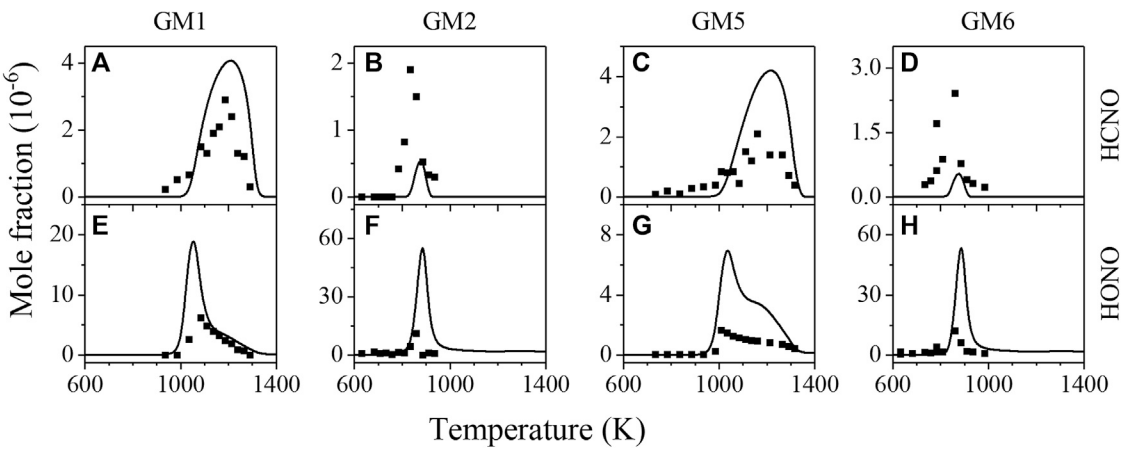

FIGURE 10 | Experimental (symbols) and simulated (lines) mole fraction profiles of HCNO and nitrous acid (HONO) in the oxidation of GM1, GM2, GM5 and GM6.

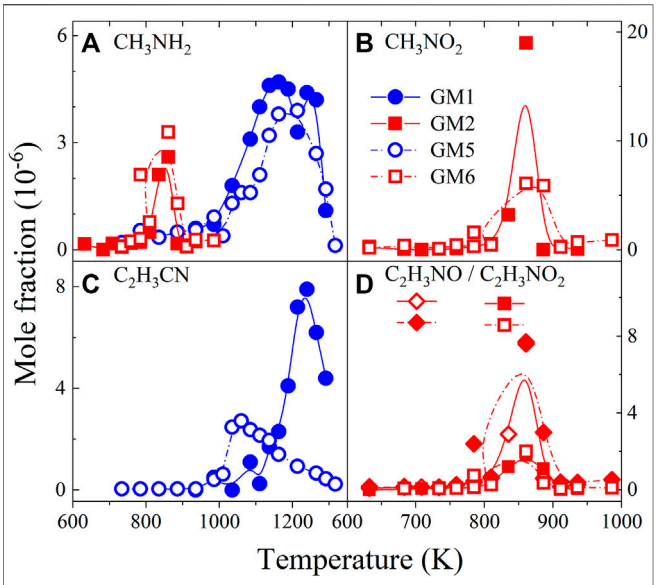

FIGURE 11 | Experimental mole fraction profiles of methylamine (CH_3NH_2), nitromethane (CH_3NO_2), vinyl cyanide (C_2H_3CN)nitrosoethylene (C_2H_3NO) and nitroethylene ($C_2H_3NO_2$) in the oxidation of GM1, GM2, GM5 and GM6.

HCNO), while the subsequent consumption of HCNO through R16 and R17 recycle NO with the dissociation of H_2NO/HNO, which complicates the process of HCNO kinetics on NO reduction.

$$HCNO + OH = H_2NO + CO \quad (R16)$$

$$HCNO + OH = HNO + HCO \quad (R17)$$

Apart from HCNO, nitrous acid (HONO) was also detected in the experiment, as seen in **Figure 10**. HONO is mainly produced from the H-abstraction reactions of CH_2CHO and H_2NO by NO_2. HONO majorly undergoes N-O bond fission to yield NO and OH, thus the HONO participated reactions belong to sensitivity reactions for the consumption of NH_3, NO, CH_4 and C_2H_4.

Figure 11 shows the measured mole fractions of CH_3NH_2, CH_3NO_2, C_2H_3CN, C_2H_3NO and $C_2H_3NO_2$ in the oxidation of GM1, GM2, GM5 and GM6. The identification of these species provides key evidence for the direct recombination reactions of CH_3, C_2H_3 with NH_2, NO_x, CN, i.e., CH_3NO_2 is the product from the reaction of CH_3 with NO_2, while C_2H_3CN is produced from the reaction of C_2H_3 with CN. Nevertheless, these species are beyond the focus of the present study, thus only a brief description is given herein.

As can be observed in **Figure 11B**, CH_3NO_2 is the most abundantly produced nitrogenous intermediates at 1 atm. CH_3NO_2 mainly decomposes to CH_2O and NO *via* CH_2NO_2 as intermediate. CH_3NH_2 can be observed at both 0.04 and 1 atm and it is mainly formed from the recombination of CH_3 with NH_2. The decomposition of CH_3NH_2 finally gives HCN *via* sequential dehydrogenation reactions $CH_3NH_2 \rightarrow CH_2NH_2 \rightarrow CH_2NH \rightarrow HCNH/H_2CN \rightarrow HCN$. The oxidation of HCN produces NO, N_2 and CO as major products under fuel-lean conditions. The decomposition of species produced from the reactions of C_2H_3, such as C_2H_3CN, C_2H_3NO and $C_2H_3NO_2$, also proceed through the stepwise H-elimination reaction, leading to the production of C_2H_2, CN and NO. C_2H_2 and CN are finally converted into CO and NO through sequential oxidation reactions. Because the consumption pathways of these nitrogenous intermediates are still not well understood, the present model is not able to reproduce their mole fraction profiles. More experimental and theoretical studies are deserved to achieve a better interpretation of the interaction kinetics between hydrocarbon radicals with NH, CN radicals and NO_x.

5 CONCLUSION

The present work has focused on two aspects with the aim to reveal the NH_3 and NO_x interaction chemistry with CH_4 and C_2H_4 at moderate temperatures and various pressures. First, speciation profiles of reactants, products, nitrogenous and oxygenated intermediates were obtained by using synchrotron vacuum ultraviolet photoionization mass spectrometry. Second, a detailed kinetic model integrating HCs/NH_3/NO_x interaction chemistry was developed and applied to interpret the experimental observations. Rate of production and sensitivity analyses were performed to analyze the conversion chemistry of NO_x and NH_3 in the presence of hydrocarbons.

The experimental results show that the addition of CH_4 and C_2H_4 promotes the conversion of NO and NH_3 at atmospheric pressure in terms of decreasing the initial conversion temperature and narrowing the reaction temperature range. The analysis results indicate that CH_4/C_2H_4 addition at atmospheric pressure promotes DeNO_x-related reactions mainly by enriching the radical pool. Besides, additional chain-branching pathways that convert NO_2 to NO are introduced due to the production of CH_3O radical. Reaction $C_2H_3 + O_2 = CH_2CHO + O$ is found to play a key role in driving the reactivity of CH_4/C_2H_4/NH_3/NO/NO_2 mixture at all the investigated conditions, generally because the further decomposition of CH_2CHO generates CH_2O, which eventually produce OH abundantly *via* the reaction sequence $CH_2O \rightarrow HCO \rightarrow HO_2 \rightarrow OH$.

The NO/NO_2 ratio is found to have only a slight impact on the conversion of CH_4, C_2H_4, NH_3 and NO from the experimental observations, while the change of pressure has significant impacts. Regarding the oxygenated and nitrogenous intermediates, formaldehyde and nitromethane are observed as the most abundantly produced oxygenated and nitrogenous intermediates, respectively. The identification of nitrogenous intermediates such as methylamine, nitromethane, vinyl cyanide, nitrosoethylene and nitroethylene provides key evidence for the direct recombination reactions of hydrocarbon or hydrocarbon radicals with NO_x, NH_2 or CN. The new data and corresponding analyses are expected to provide valuable information for understanding the complex gas phase reactions in the exhaust gas as well as an extension of the kinetic model of HCs/NH_3/NO_x reaction systems.

DATA AVAILABILITY STATEMENT

The raw data supporting the conclusions of this article will be made available by the authors, without undue reservation.

AUTHOR CONTRIBUTIONS

YD: Methodology, Investigation, Data curation, Writing- original draft. ZS: Methodology, Investigation, Data curation. WY: Conceptualization, Methodology, Writing -review and editing, Funding acquisition. JY: Methodology, investigation. ZZ: Methodology, Writing - review and editing. FQ: Funding acquisition, Writing - review and editing.

FUNDING

The authors are grateful for the funding support from the National Natural Science Foundation of China (51706137, 51761135111) and the National Key R&D Program of China (2019YFA0405602).

ACKNOWLEDGMENTS

The authors wish to acknowledge the financial support provided by the National Natural Science Foundation of China.

REFERENCES

Alzueta, M., Ara, L., Mercader, V., Delogu, M., and Bilbao, R. (2021). Interaction of NH_3 and NO under Combustion Conditions. Experimental Flow Reactor Study and Kinetic Modeling Simulation. *Combustion and Flame* 235, 111691. doi:10.1016/j.combustflame.2021.111691

Börnhorst, M., and Deutschmann, O. (2021). Advances and Challenges of Ammonia Delivery by Urea-Water Sprays in SCR Systems. *Prog. Energ. Combustion Sci.* 87, 100949. doi:10.1016/j.pecs.2021.100949

Deng, F., Zhang, Y., Sun, W., Huang, W., Zhao, Q., Qin, X., et al. (2019). Towards a Kinetic Understanding of the NOx Sensitization Effect on Unsaturation Hydrocarbons: A Case Study of Ethylene/nitrogen Dioxide Mixtures. *Proc. Combustion Inst.* 37 (1), 719–726. doi:10.1016/j.proci.2018.07.115

Duynslaegher, C., Contino, F., Vandooren, J., and Jeanmart, H. (2012). Modeling of Ammonia Combustion at Low Pressure. *Combustion and Flame* 159 (9), 2799–2805. doi:10.1016/j.combustflame.2012.06.003

Gasnot, L., Dao, D. Q., and Pauwels, J. F. (2012). Experimental and Kinetic Study of the Effect of Additives on the Ammonia Based SNCR Process in Low Temperature Conditions. *Energy Fuels* 26 (5), 2837–2849. doi:10.1021/ef300310c

Glarborg, P., Miller, J. A., Ruscic, B., and Klippenstein, S. J. (2018). Modeling Nitrogen Chemistry in Combustion. *Prog. Energ. Combustion Sci.* 67, 31–68. doi:10.1016/j.pecs.2018.01.002

Hemberger, R., Muris, S., Pleban, K.-U., and Wolfrum, J. (1994). An Experimental and Modeling Study of the Selective Noncatalytic Reduction of NO by Ammonia in the Presence of Hydrocarbons. *Combustion and Flame* 99 (3-4), 660–668. doi:10.1016/0010-2180(94)90060-4

Hutter, R., De Libero, L., Elbert, P., and Onder, C. H. (2018). Catalytic Methane Oxidation in the Exhaust Gas Aftertreatment of a Lean-Burn Natural Gas Engine. *Chem. Eng. J.* 349, 156–167. doi:10.1016/j.cej.2018.05.054

Jia, Y., Jiang, J., Zheng, R., Guo, L., Yuan, J., Zhang, S., et al. (2021). Insight into the Reaction Mechanism over PMoA for Low Temperature NH3-SCR: A Combined *In-Situ* DRIFTs and DFT Transition State Calculations. *J. Hazard. Mater.* 412, 125258. doi:10.1016/j.jhazmat.2021.125258

Johnson, T. V. (2015). Review of Vehicular Emissions Trends. *SAE Int. J. Engines* 8 (3), 1152–1167. doi:10.4271/2015-01-0993

Lee, K., Choi, B., Lee, C., and Oh, K. (2020). Effects of SiO2/Al2O3 Ratio, Reaction Atmosphere and Metal Additive on De-NOx Performance of HC-SCR over Cu-Based ZSM-5. *J. Ind. Eng. Chem.* 90, 132–144. doi:10.1016/j.jiec.2020.07.005

Lott, P., and Deutschmann, O. (2021). Lean-Burn Natural Gas Engines: Challenges and Concepts for an Efficient Exhaust Gas Aftertreatment System. *Emiss. Control. Sci. Technol.* 7 (1), 1–6. doi:10.1007/s40825-020-00176-w

Marshall, P., Leung, C., Gimenez-Lopez, J., Rasmussen, C. T., Hashemi, H., Glarborg, P., et al. (2019). The C2H2 + NO2 Reaction: Implications for High Pressure Oxidation of C2H2/NOx Mixtures. *Proc. Combustion Inst.* 37 (1), 469–476. doi:10.1016/j.proci.2018.06.202

Mejía-Centeno, I., Castillo, S., Camposeco, R., and Fuentes, G. A. (2013). SCR of NOx by NH3 over Model Catalysts: The Kinetic Data-Linear Free Energy Relation. *Catal. Commun.* 31, 11–15. doi:10.1016/j.catcom.2012.10.022

Miller, J. A., and Bowman, C. T. (1989). Mechanism and Modeling of Nitrogen Chemistry in Combustion. *Prog. Energ. Combustion Sci.* 15 (4), 287–338. doi:10.1016/0360-1285(89)90017-8

Okafor, E. C., Naito, Y., Colson, S., Ichikawa, A., Kudo, T., Hayakawa, A., et al. (2018). Experimental and Numerical Study of the Laminar Burning Velocity of CH4-NH3-air Premixed Flames. *Combustion and flame* 187, 185–198. doi:10.1016/j.combustflame.2017.09.002

Piumetti, M., Bensaid, S., Fino, D., and Russo, N. (2016). Catalysis in Diesel Engine NOxaftertreatment: a Review. *Catal. Struct. Reactivity* 1 (4), 155–173. doi:10.1080/2055074x.2015.1105615

Qi, F. (2013). Combustion Chemistry Probed by Synchrotron VUV Photoionization Mass Spectrometry. *Proc. Combustion Inst.* 34 (1), 33–63. doi:10.1016/j.proci.2012.09.002

ReactionDesign (2009). *CHEMKIN-PRO 15092 Reaction Design*. San Diego 2009.

Sahu, A. B., Mohamed, A. A. E.-S., Panigrahy, S., Saggese, C., Patel, V., Bourque, G., et al. (2021). An Experimental and Kinetic Modeling Study of NO_x Sensitization on Methane Autoignition and Oxidation. *Combustion and Flame*, 111746. doi:10.1016/j.combustflame.2021.111746

Savva, Z., Petallidou, K. C., Damaskinos, C. M., Olympiou, G. G., Stathopoulos, V. N., and Efstathiou, A. M. (2021). H_2-SCR of NO_x on Low-SSA CeO_2-Supported Pd: The Effect of Pd Particle Size. *Appl. Catal. A: Gen.* 615, 118062. doi:10.1016/j.apcata.2021.118062

Schmitt, S., Schwarz, S., Ruwe, L., Horstmann, J., Sabath, F., Maier, L., et al. (2021). Homogeneous Conversion of NO X and NH 3 with CH 4 , CO, and C 2 H 4 at the Diluted Conditions of Exhaust-gases of Lean Operated Natural Gas Engines. *Int. J. Chem. Kinet.* 53 (2), 213–229. doi:10.1002/kin.21435

Srinivasan, N. K., Su, M.-C., Sutherland, J. W., and Michael, J. V. (2005). Reflected Shock Tube Studies of High-Temperature Rate Constants for OH + CH4 → CH3 + H2O and CH3 + NO2 → CH3O + NO. *J. Phys. Chem. A.* 109 (9), 1857–1863. doi:10.1021/jp040679j

Stagni, A., Cavallotti, C., Arunthanayothin, S., Song, Y., Herbinet, O., Battin-Leclerc, F., et al. (2020). An Experimental, Theoretical and Kinetic-Modeling Study of the Gas-phase Oxidation of Ammonia. *React. Chem. Eng.* 5 (4), 696–711. doi:10.1039/C9RE00429G

Sumathi, R., Sengupta, D., and Nguyen, M. T. (1998). Theoretical Study of the H2 + NO and Related Reactions of [H2NO] Isomers. *J. Phys. Chem. A.* 102 (18), 3175–3183. doi:10.1021/jp9804953

Sun, Z., Deng, Y., Song, S., Yang, J., Yuan, W., and Qi, F. (2021). Experimental and Kinetic Modeling Study of the Homogeneous Chemistry of NH_3 and NO_x with CH_4 at the Diluted Conditions. *Combustion and Flame, submitted*.

Tamm, S., Ingelsten, H. H., Skoglundh, M., and Palmqvist, A. E. C. (2009). The Influence of Gas Phase Reactions on the Design Criteria for Catalysts for Lean NO_x Reduction with Dimethyl Ether. *Appl. Catal. B: Environ.* 91 (1-2), 234–241. doi:10.1016/j.apcatb.2009.05.030

Torkashvand, B., Lott, P., Zengel, D., Maier, L., Hettel, M., Grunwaldt, J.-D., et al. (2019). Homogeneous Oxidation of Light Alkanes in the Exhaust of Turbocharged Lean-Burn Gas Engines. *Chem. Eng. J.* 377, 119800. doi:10.1016/j.cej.2018.08.186

Vassallo, J., Miró, E., and Petunchi, J. (1995). On the Role of Gas-phase Reactions in the Mechanism of the Selective Reduction of NO_x. *Appl. Catal. B: Environ.* 7 (1-2), 65–78. doi:10.1016/0926-3373(95)00032-1

Wang, D., Peng, Y., Yang, Q., Hu, F., Li, J., and Crittenden, J. (2019). NH3-SCR Performance of WO3 Blanketed CeO2 with Different Morphology: Balance of Surface Reducibility and Acidity. *Catal. Today* 332, 42–48. doi:10.1016/j.cattod.2018.07.048

Yamaguchi, Y., Teng, Y., Shimomura, S., Tabata, K., and Suzuki, E. (1999). Ab Initio Study for Selective Oxidation of Methane with NOx (X = 1, 2). *J. Phys. Chem. A.* 103 (41), 8272–8278. doi:10.1021/jp990985a

Zhou, C.-W., Li, Y., Burke, U., Banyon, C., Somers, K. P., Ding, S., et al. (2018). An Experimental and Chemical Kinetic Modeling Study of 1,3-butadiene Combustion: Ignition Delay Time and Laminar Flame Speed Measurements. *Combustion and Flame* 197, 423–438. doi:10.1016/j.combustflame.2018.08.006

Zhou, Z., Du, X., Yang, J., Wang, Y., Li, C., Wei, S., et al. (2016). The Vacuum Ultraviolet Beamline/endstations at NSRL Dedicated to Combustion Research. *J. Synchrotron Radiat.* 23 (4), 1035–1045. doi:10.1107/S1600577516005816

Conflict of Interest: The authors declare that the research was conducted in the absence of any commercial or financial relationships that could be construed as a potential conflict of interest.

Publisher's Note: All claims expressed in this article are solely those of the authors and do not necessarily represent those of their affiliated organizations, or those of the publisher, the editors and the reviewers. Any product that may be evaluated in this article, orclaim that may be made by its manufacturer, is not guaranteed or endorsed by the publisher.